Variable-force microscopy for advanced characterization of horizontally aligned carbon nanotubes

2011 Nanotechnology 22 275717

(http://iopscience.iop.org/0957-4484/22/27/275717)

Nanotechnology **22** (2011) 275717 (5pp) doi:10.1088/0957-4484/22/27/275717

Variable-force microscopy for advanced characterization of horizontally aligned carbon nanotubes

Ali A Almaqwashi, Joshua W Kevek, Rachel M Burton, Tristan DeBorde and Ethan D Minot

Department of Physics, Oregon State University, Corvallis, OR, USA

E-mail: minote@science.oregonstate.edu

Received 12 January 2011, in final form 4 May 2011
Published 26 May 2011
Online at stacks.iop.org/Nano/22/275717

Abstract

Atomic force microscopy (AFM) performed with variable-force imaging was recently demonstrated to be an accurate method of determining the diameter and number of sidewalls of a carbon nanotube (CNT). This AFM technique provides an alternative to transmission electron microscopy (TEM) when TEM imaging is not possible due to substrate thickness. We have used variable-force AFM to characterize horizontally aligned CNTs grown on ST-cut quartz. Our measurements reveal new aspects of horizontally aligned growth that are essential for enhancing the performance of CNT-based devices as well as understanding the growth mechanism. First, previously reported optimal growth conditions produce a large spread in CNT diameters and a significant fraction of double-walled CNTs. Second, monodispersity is significantly improved when growth temperature is reduced. Third, CNTs with diameters up to 5 nm align to the substrate, suggesting the interaction between CNTs and the quartz lattice is more robust than previously reported.

(Some figures in this article are in colour only in the electronic version)

1. Introduction

Recent breakthroughs in chemical vapor deposition (CVD) techniques for synthesizing carbon nanotubes (CNTs) have led to high-yield, large-scale integration of CNT transistors [1, 2]. The use of crystalline substrates such as quartz has enabled high-density growth of horizontally aligned CNTs [2, 3]. Further improvements to growth recipes have enabled selective growth of semiconducting CNTs on quartz [4], and complementary efforts to scale up CNT production have shown that 4 inch wafers can be coated with high-density horizontally aligned CNTs [5].

Obtaining monodisperse diameter distributions of horizontally aligned CNTs is critical for high performance nanoelectronics [1, 6]. The semiconductor bandgap, electron and hole effective masses and other electronic properties change with CNT diameter [7]. Accurate determination of CNT diameter is possible with transmission electron microscopy (TEM) or resonant Raman spectroscopy measurements of the radial breathing mode. Due to the technical challenge of transferring CNTs from a quartz substrate to a TEM grid, TEM has not been used to study the distribution of CNTs obtained using substrate-aligned growth. Resonant Raman studies of CNTs grown on quartz have been performed [4], but these previous measurements lacked single-CNT resolution and only detected a fraction of CNTs (i.e. CNTs that were resonant with the laser excitation wavelength). Atomic force microscopy (AFM) is typically used to measure diameter distributions of horizontally aligned CNTs, but previous investigators have not controlled the magnitude of imaging forces. Reports of diameter distributions vary from 2 ± 1 nm to 0.8 ± 0.2 nm [1, 4, 8]. These differences may be the result of different CVD growth recipes, or may be due to differences in AFM imaging forces since imaging forces are known to cause radial compression of CNTs [9, 10].

In our current work we use a variable-force AFM imaging technique, first introduced by DeBorde *et al* [9], to characterize and optimize the monodispersity of horizontally aligned growth on quartz. This AFM technique provides advanced characterization while circumventing the problem that TEM

imaging is not possible on thick substrates. By tuning the CNT growth temperature and the thickness of the growth catalyst, we demonstrate significant improvements in monodispersity of horizontally aligned CNTs on quartz.

2. Sample preparation

Horizontally aligned CNTs were grown on ST-cut quartz substrate (Hoffman Materials) in a CVD growth system (Kevek Innovations) following procedures originally developed by Kocabas *et al* and Ding *et al* [2, 4]. Photolithography was used to pattern catalyst stripes (10 μm wide, 100 μm spacing for Batch 1, and 5 μm wide, 50 μm spacing for Batch 2). Electron-beam evaporation was used to deposit Fe at two different thicknesses, $t_{cat} = 0.2$ nm for Batch 1, and 1.5 nm for Batch 2. Prior to the growth runs, the catalyst-coated quartz chips were annealed for 1 h at 800 °C with (0.45 standard liters per minute (SLM)) hydrogen flow and then cooled to room temperature. The growth process had three parts: (i) annealing in hydrogen for 15 min at 800 °C, (ii) a temperature ramp to reach our target growth temperature (T_{growth}), and (iii) a 15 min exposure to alcohol vapor while temperature was held at T_{growth}. Throughout the entire process a flow of 0.45 SLM of hydrogen was maintained. The alcohol vapor was a mixture of ethanol and methanol vapor created by bubbling argon through ice-cold alcohol. Argon was bubbled through the ethanol at a rate of 0.15 SLM and through the methanol at 0.3 SLM [4]. Six different growth runs were performed using $t_{cat} = 0.2$ nm (T_{growth} varied from 700 to 950 °C, all other parameters were fixed). Nanotubes did not grow for $T_{growth} < 800$ °C. Five different growth runs were performed using $t_{cat} = 1.5$ nm (T_{growth} varied from 800 to 900 °C, all other parameters were fixed).

3. Results and discussion

Figure 1 shows height measurements of three CNTs obtained using two different imaging forces. Our choice of imaging parameters, and interpretation of the resulting images, are based on the work of DeBorde *et al* [9] and similar work by Barboza *et al* [11]. Carbon nanotube diameters are much smaller than the radius of curvature of standard AFM tips (we have used tips with radius of curvature ranging from 30 to 60 nm). Therefore, the lateral dimensions of the CNTs are not resolved and we focus on the height dimension. The low-force image was obtained using a tapping amplitude of 11 nm and a set point amplitude of 6 nm. The phase of cantilever oscillation (relative to the driving force) was >90°, indicating attractive mode imaging. DeBorde *et al* estimate the tapping force for these conditions to be approximately 1 nN which corresponds to a gentle imaging force and minimizes radial compression. A high-force image of the same area was obtained using a tapping amplitude of 100 nm and a set point amplitude of 50 nm. The phase of cantilever oscillation (relative to the driving force) was <90°, indicating repulsive mode imaging. The estimated tapping force for these conditions is about 50 nN. This imaging force is sufficient to compress individual single-walled CNTs (SWCNTs) to a thickness between 0.4 and

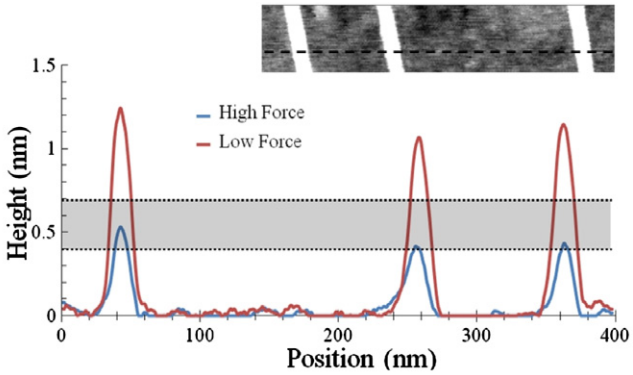

Figure 1. Three CNTs imaged with low and high forces (approximately 1 nN and 50 nN respectively). The sample was grown at $T_{growth} = 800$ °C. The AFM cantilever has nominal spring constant of 40 N m^{-1}. The shaded range, 0.4–0.7 nm, shows the expected height of SWCNTs measured with the high imaging force. The inset shows the low-force AFM image, the scan size is 400 nm × 120 nm.

0.7 nm. This imaging force is insufficient to fully compress bundles of SWCNTs (multiple SWCNTs that form a single object) as shown in figure 2. Multi-walled CNTs also appear taller than 0.7 nm in high-force images. In summary, high-force measurements identify individual SWCNTs, while low-force measurements report the CNT diameters [9].

The low-force imaging parameters described above were used to measure diameter distributions for all 11 growth runs. For each growth run we also characterized the degree of CNT alignment and the growth density using standard AFM imaging. For a subset of growth runs we determined the ratio of SWCNTs to non-single-walled CNTs by using the high-force imaging parameters described above. All imaging was done 5 μm from the edge of the catalyst where the majority (>98%) of CNTs were aligned to the preferential growth direction. Only aligned CNTs are included in our analysis.

We imaged a total of 202 CNTs and found that 199 of these CNTs were aligned to the X-axis of the quartz substrate. This large number of aligned CNTs included 87 CNTs with diameters between 1.5 and 5.5 nm. A previous study showed that CNTs with diameters greater than 1.5 nm are unlikely to align to Y-cut quartz substrates [2]. Our current observations of CNTs on ST-cut quartz show that CNT alignment is more robust on ST-cut quartz substrates.

Next we examine the measurements of CNTs grown from $t_{cat} = 0.2$ nm at $T_{growth} = 825$ °C. Figure 3 shows the distributions of nanotube heights measured first with low force (figure 3(a)) and then with high force (figure 3(b)). Following DeBorde *et al*, we interpret figure 3(a) as an accurate representation of the diameter distribution, while figure 3(b) is interpreted as a height distribution of squashed CNTs. Nanotubes which are compressed to heights below 0.7 nm are identified as single-walled (0.7 nm is the nominal thickness of two atomic layers of graphite) [9]. Based on the fraction of CNTs with compressed heights below 0.7 nm we estimate that at least 60% of the CNTs in this sample are single walled. A small fraction of the CNTs that are included in our analysis (∼4%) were clearly bundles, as evidenced by Y junctions

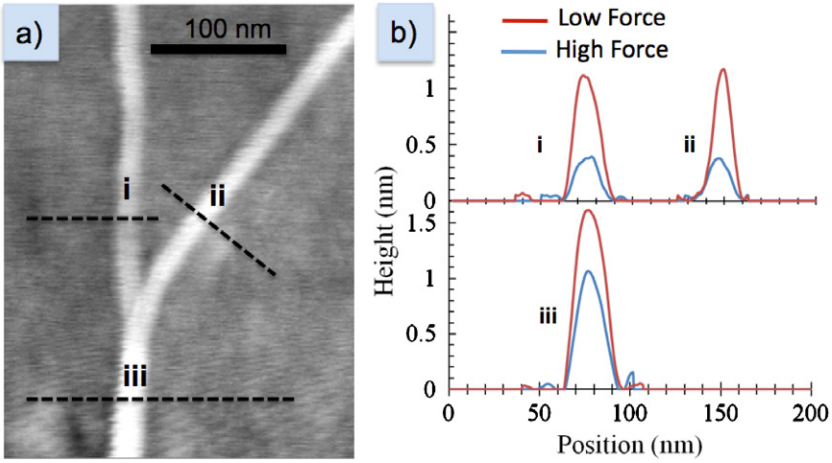

Figure 2. Variable-force AFM measurements of CNTs forming a bundle. (a) Low-force image of two CNTs (upper half) and a bundle (lower half). (b) Cross-sectional analysis of low-force and high-force images at positions (i)–(iii). The isolated CNTs at position (i) and (ii) are both about 1.1 nm tall in the low-force image, and compress to 0.4 nm in the high-force image. The CNT bundle at position (iii) is 1.6 nm tall in the low-force image and compresses to 1.0 nm in the high-force image.

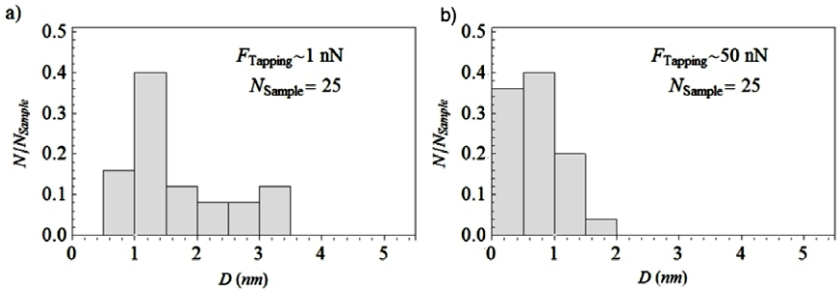

Figure 3. Apparent height of CNTs grown at 825 °C, measured with low-force and high-force imaging; (a) low tapping force and (b) high tapping force. The distribution obtained by high-force imaging gives the misleading impression that all CNTs have diameter less than 2 nm.

where two CNTs bundled together (see figure 2). Bundles require higher forces for full radial compression, therefore, high-force imaging does not identify single-walled CNTs that are part of bundles. The presence of bundles will lead to a small error (∼4%) in our estimate of the SWCNT fraction.

An important conclusion from figure 3 is that imaging forces have a significant impact on AFM measurements of CNT diameter distributions. If our high-force images are misinterpreted as faithful measurements of CNT diameter, the resulting diameter distribution (figure 3(b)) would lead to false conclusions about monodispersity.

We now turn to the effect of T_{growth} on the distribution of CNT diameters. Figure 4 shows the diameter distributions (obtained from low-force imaging) of CNTs grown at different T_{growth} using $t_{cat} = 0.2$ nm. It is clear that lower T_{growth} yields smaller diameter CNTs and better monodispersity. At $T_{growth} = 800\,°C$ the average diameter is $D_{avg} = 1.1$ nm, standard deviation $\sigma = 0.28$ nm and the fraction of SWCTs is at least 73%. At $T_{growth} = 900\,°C$ we found $D_{avg} = 2.0$ nm, $\sigma = 1.2$ nm, and only 46% SWCNTs. The thicker catalyst ($t_{cat} = 1.5$ nm) showed similar trends in D_{avg} and σ as a function of T_{growth} (histograms not shown).

Our observation that lower T_{growth} favors the growth of smaller diameter horizontally aligned CNTs is consistent with previous studies of laser-ablation growth [12] and non-aligned CVD growth on SiO_2 [6]. Our current measurements confirm that the temperature-dependency also occurs for horizontally aligned CNTs. Common explanations for temperature-dependent diameter distributions are based on the relationship between CNT diameter and the size of the catalyst particle [8]. Lower T_{growth} is thought to favor CNT growth from smaller catalyst particles for two reasons: (i) large diameter catalyst particles are not activated at low temperature because the catalyst melting point and carbon solubility depend on the diameter of the catalyst particle, (ii) Ostwald ripening of catalyst particles is less pronounced at low temperatures, favoring the formation of smaller catalyst particles.

The thickness of the evaporated iron catalyst, t_{cat}, affected monodispersity at low T_{growth} but did not affect monodispersity at higher growth temperatures. For the growth conditions (800 °C, $t_{cat} = 0.2$ nm) we found $D_{avg} = 1.1$ nm, $\sigma = 0.28$ nm. For the growth conditions (800 °C, $t_{cat} = 1.5$ nm) we found $D_{avg} = 1.1$ nm, $\sigma = 0.40$ nm. The lower value of σ for the thin catalyst indicates better monodispersity. For high temperature growth conditions 900 °C, $t_{cat} = 0.2$ nm

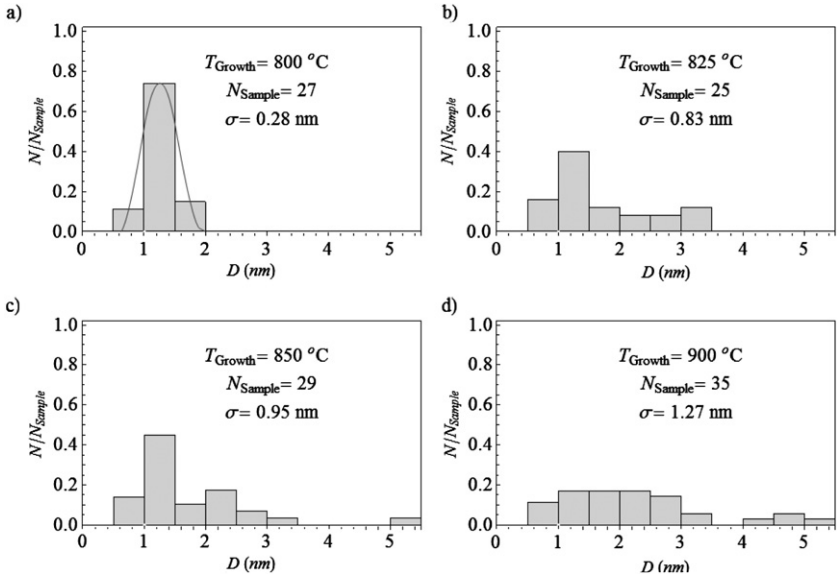

Figure 4. Diameter distributions from CNT samples grown at several growth temperatures from 800 to 900 °C using a thin catalyst (0.2 nm). The monodispersity improves at lower T_{growth} (measured by the standard deviation σ). The same trend was found using thicker catalyst (histograms not shown).

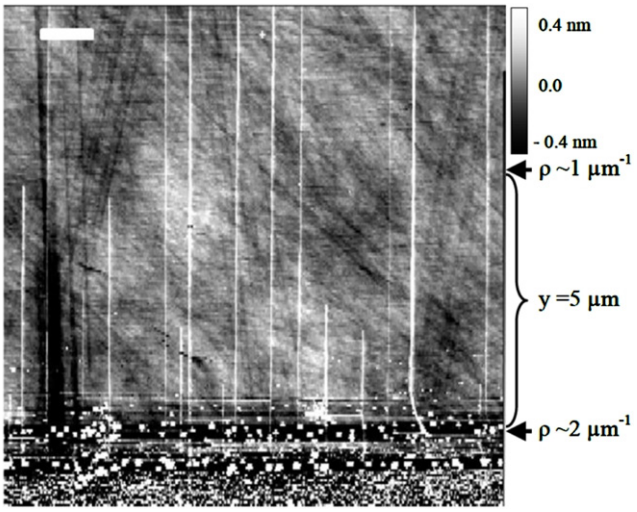

Figure 5. The AFM image for a growth run at 800 °C shows horizontally aligned CNTs reaching different lengths from the Fe catalyst. At 5 μm away from the catalyst edge the density dropped by 50%. The scale bar is 1 μm.

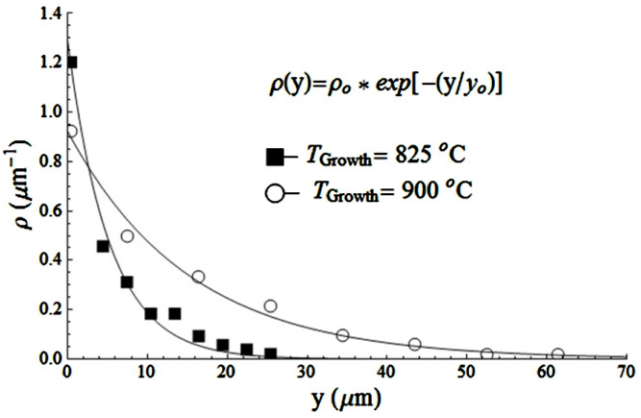

Figure 6. The density of CNTs is measured at several distances from the catalyst. The density (ρ) drops exponentially over distance (y); rapidly for lower temperature (825 °C, the solid squares) and gradually for higher temperature (900 °C, the circles). The solid lines are exponential fits with decay constants $y_o = 5$ μm and 15 μm respectively.

and 900 °C, $t_{cat} = 1.5$ nm we found $D_{avg} = 2.0$ nm, $\sigma = 1.2$ nm in both cases. In summary, of the growth conditions tested, the optimal choice for monodisperse SWCNTs was $T_{growth} = 800$ °C and $t_{cat} = 0.2$ nm. These parameters are significantly different from optimal conditions previously reported in the literature for horizontally aligned CNTs grown from evaporated iron films (T_{growth} ranging from 875 to 950 °C [13–16]).

Horizontally aligned CNTs grow to different lengths, as shown in figure 5, and the average length depends on growth temperature. This effect was investigated by measuring the length distribution for CNTs grown at 825 and 900 °C. We quantified the linear density of horizontally aligned CNTs, ρ, following the usual convention [14]. A reference line is drawn perpendicular to the growth direction; ρ is the number CNTs crossing the line, divided by the length of the line. Figure 6 illustrates how ρ decreases as a function of distance (y) from the catalyst edge. Although growth temperature did not significantly affect the density of CNTs at the catalyst edge ($\rho_o \sim 1$ μm^{-1} for both growth temperatures), the density drops more rapidly with distance for the lower growth temperature. The experimental data are described well by exponential fits with characteristic decay lengths of $y_o = 5$ μm ($T_{growth} = 825$ °C) and $y_o = 15$ μm ($T_{growth} = 900$ °C). The exponential decay of CNT density seen in figure 6 is consistent with previous studies of gas-flow-aligned

CNTs [17]. A deeper understanding of the temperature-dependent mechanisms affecting the length of horizontally aligned CNTs would be useful for the optimization of growth of monodisperse SWCNTs at 800 °C.

4. Conclusion

We conclude that variable-force imaging is a valuable tool for accurately characterizing CNT growth, particularly when transmission electron microscopy is not possible or practical. We have illustrated the utility of this characterization technique by identifying growth conditions ($T_{\text{growth}} = 800\,^{\circ}\text{C}$ and $t_{\text{cat}} = 0.2$ nm) that significantly improve the monodispersity of CNTs grown from evaporated iron catalyst on ST-cut quartz. This enhanced monodispersity will be useful for improving the homogeneity/performance of CNT-based devices. Lower growth temperatures deserve further study to explore the possibility of optimizing CNT length while preserving a monodisperse diameter distribution.

Acknowledgments

This work was supported by the Office of Naval Research through the Oregon Nanoscience and Microtechnology Institute. A portion of the sample fabrication was performed at the Cornell node of the National Nanofabrication Infrastructure Network, which is supported by the National Science Foundation (Grant ECS-0335765).

References

[1] Kang S *et al* 2007 High-performance electronics using dense, perfectly aligned arrays of single-walled carbon nanotubes *Nat. Nanotechnol.* **2** 230–6

[2] Kocabas C *et al* 2005 Guided growth of large-scale, horizontally aligned arrays of single-walled carbon nanotubes and their use in thin-film transistors *Small* **1** 1110–6

[3] Xiao J *et al* 2009 Alignment controlled growth of single-walled carbon nanotubes on quartz substrates *Nano Lett.* **9** 4311–9

[4] Ding L *et al* 2009 Selective growth of well-aligned semiconducting single-walled carbon nanotubes *Nano Lett.* **9** 800–5

[5] Ryu K *et al* 2009 CMOS-analogous wafer-scale nanotube-on-insulator approach for submicrometer devices and integrated circuits using aligned nanotubes *Nano Lett.* **9** 189

[6] Mudimela P *et al* 2009 Incremental variation in the number of carbon nanotube walls with growth temperature *J. Phys. Chem.* C **113** 2212–8

[7] Javey A 2009 Carbon nanotube field-effect transistors *Carbon Nanotube Electronics* ed A Javey and J Kong (New York: Springer) pp 1–24

[8] Lu C and Liu J 2006 Controlling the diameter of carbon nanotubes in chemical vapor deposition method by carbon feeding *J. Phys. Chem.* B **110** 20254–7

[9] DeBorde T *et al* 2008 Identifying individual single-walled and double-walled carbon nanotubes by atomic force microscopy *Nano Lett.* **8** 3568–71

[10] Postma H, Sellmeijer A and Dekker C 2000 Manipulation and imaging of individual single-walled carbon nanotubes with an atomic force microscope *Adv. Mater.* **12** 1299–302

[11] Barboza A, Chacham H and Neves B 2009 Universal response of single-wall carbon nanotubes to radial compression *Phys. Rev. Lett.* **102** 25501

[12] Bandow S *et al* 1998 Effect of the growth temperature on the diameter distribution and chirality of single-wall carbon nanotubes *Phys. Rev. Lett.* **80** 3779–82

[13] Hart A, Slocum A and Royer L 2006 Growth of conformal single-walled carbon nanotube films from Mo/Fe/Al_2O_3 deposited by electron beam evaporation *Carbon* **44** 348–59

[14] Hong S W, Banks T and Rogers J A 2010 Improved density in aligned arrays of single walled carbon nanotubes by sequential chemical vapor deposition on quartz *Adv. Mater.* **22** 1826–30

[15] Liu H *et al* 2009 The controlled growth of horizontally aligned single-walled carbon nanotube arrays by a gas flow process *Nanotechnology* **20** 345604

[16] Akinwande D *et al* 2009 Surface science of catalyst dynamics for aligned carbon nanotube synthesis on a full-scale quartz wafer *J. Phys. Chem.* C **113** 8002–8

[17] Zheng L *et al* 2009 Kinetics studies of ultralong single-walled carbon nanotubes *J. Phys. Chem.* C **113** 10896–900